Advanced and Sustainable Technologies (ASET) eISSN 2976-2294
Volume 1, No 2, December 2022 [76-86]

Effects of Cutouts on Energy Absorption Characteristics of Thin-walled Tube Impacted under Dynamic Loading

M. H. Zikri[1], M. Ahmad[1*], M. N. Misbah[1], M. H. M. Hazwan[1], A. H. M. Haidiezul[1], M.A.M. Nawi[1] and W. M. Faizal[1]

[1]Faculty of Mechanical Engineering & Technology, Universiti Malaysia Perlis, Pauh Putra Campus, 02600, Arau, Perlis, Malaysia.

Received 15 Nov 2022, Revised 22 Nov 2022, Accepted 30 Nov 2022

ABSTRACT

A thin-walled tube is an energy absorber device that is commonly used in automotive and locomotive applications. The function of this element is to convert the kinetic energy into other forms of energy during a collision that can minimize injuries to the passengers. Therefore, various studies have been reported previously to improve the thin-walled structure to decrease the damage and provide protection for the vehicle and occupant. This study aims to determine the effects of the cutout on the thin-walled tube when impacted under dynamic axial loading. The effects of sizes, shapes, locations, and the number of cutouts on the energy absorption characteristics have been analyzed by using the validated finite element model. The result indicates that a circular tube with a square cutout shape, larger cutout sizes, and near the top-end of the tube has more energy absorption characteristics. Furthermore, the results of energy absorption (EA), crush force efficiency (CFE), and specific energy absorption (SEA) are highest when applying four cutouts on the surface of the thin-walled tube. Research information provided in this study will serve as a guide in designing the cutout thin-walled tube for crashworthiness enhancements in the future.

Keywords: Thin-walled tubes, Energy absorber, Crashworthiness, Imperfection tubes, Finite element model.

1. INTRODUCTION

The thin-walled tube is the most common type of collapsible energy absorption used to absorb the kinetic energy and dissipate it into the other forms of energy during an impact event. The thin-walled tube plays a significant role in absorbing the impact energy and reducing initial peak force to minimize passenger acceleration. The performance of the thin-walled tubes is always analyzed by the crashworthiness criteria such as total energy absorption, initial peak crushing, mean crushing load, crush force efficiency, specific energy absorption, and many more.

According to the World Health Organization, road traffic accidents are the greatest killer of children and young people globally, resulting in an estimated 50 million injuries and about 1.3 million avoidable fatalities annually [1]. A safer transport system with increased crashworthiness resistance is thus a daily necessity. Researchers, automotive engineers, and designers have tried to reduce the effect of load through several energy absorption mechanisms. These can be done by varying the material, structural geometry, and loading modes which are the key factors influencing the energy absorption ability of thin-walled components [2-3].

Numerous geometries and modifications of the thin-walled tubes have been introduced in previous literature [4]. The geometries of the tubes varied from the conventional type, such as

*Corresponding author: masniezam@unimap.edu.my

circular [5] and square tube [6] until the complex geometries, such as multi-cell [7] and corrugated tubes [8]. Furthermore, adding filler into the tubes improves the structure's crashworthiness [9]. It was also discovered that tubes with patterned holes, also known as cutout tubes, significantly increased the efficiency of energy absorption characteristics [10-11]. For example, the cutout tube that collapsed in an extensional mode has a better energy absorption capacity, up to 23 % greater than the conventional tube [12]. When different types of tubes were tested, it was discovered that the energy absorption characteristics of tubes with circular cutouts were superior to those with square and trapezoidal cutouts tubes [11]. In terms of initial peak load, it was found that the value of the initial peak load of the cutout tube can be reduced by up to 63 % compared to the conventional tube [12]. These results affected the crush force efficiency (CFE), where the optimal CFE of the tubes with lateral circular cuts was 27.4 % bigger than the conventional tube [10]. Besides that, most cutout tubes have a higher specific energy absorption (SEA) than conventional tubes. Compared to tubes without cutouts, the optimal SEA of the tubes with cutouts can be increased up to 26.4 % [10] and 54 % [12]. The literature studies mentioned above reveal those investigations into how the size and shape of cutouts affect changes in energy absorption characteristics. However, the studies on the effect of cutout still need more attention as various types of shapes, sizes and numbers of cutouts can be formed on the thin-walled tube.

This study aims to investigate the characteristics of energy absorption impacted under dynamic loading of the cutout tube with different locations, numbers, and shapes. A finite element model has been used to simulate the cutout tubes under axial impact loading. The model has been verified with previous experimental works. The results of energy absorption characteristics, such as energy absorption capacity, initial peak load, SEA, and CFE, are discussed in the following sections.

2. MATERIAL AND METHODS

Several parametric studies were conducted to determine the performance of energy absorption characteristics of thin-walled tubes under different conditions. Table 1 shows all the parameters used in this study. Two types of cross-sections of thin-walled tubes have been used, which are circular and square straight tubes. Aluminum alloy AA 6061-T6 has been used as the material for all specimens, with the length, thickness, and diameter kept constant at 150 mm, 0.58 mm, and 50 mm, respectively. All tubes were impacted under axial dynamic loading with 20 m/s of initial impact speed.

2.1 Details of parametric studies

In investigating the effects of cutout shape and size, three cutout geometries have been used: circular, square, and hexagon, as shown in Figure 1. The diameter of these cutouts varied from 14 mm, 20 mm, and 25 mm. The cutout was also created at the top, middle, and bottom locations. Thus, the effect of cutout location on the results can be measured. Apart from that, the number of cutouts in a single tube varied from 1 to 5 holes along the tube has also been conducted.

Table 1: Parameters of thin-walled tube and cutout profiles.

Tube shape	Length (mm)	Thickness (mm)	Diameter (mm)	Impact speed (m/s)	Cutout shape	Cutout location	Cutout diameter (mm)	Number of cutouts
Circular Square	150	0.58	50	20	Circular Square Hexagon	Top Middle Bottom	14 20 25	1-5

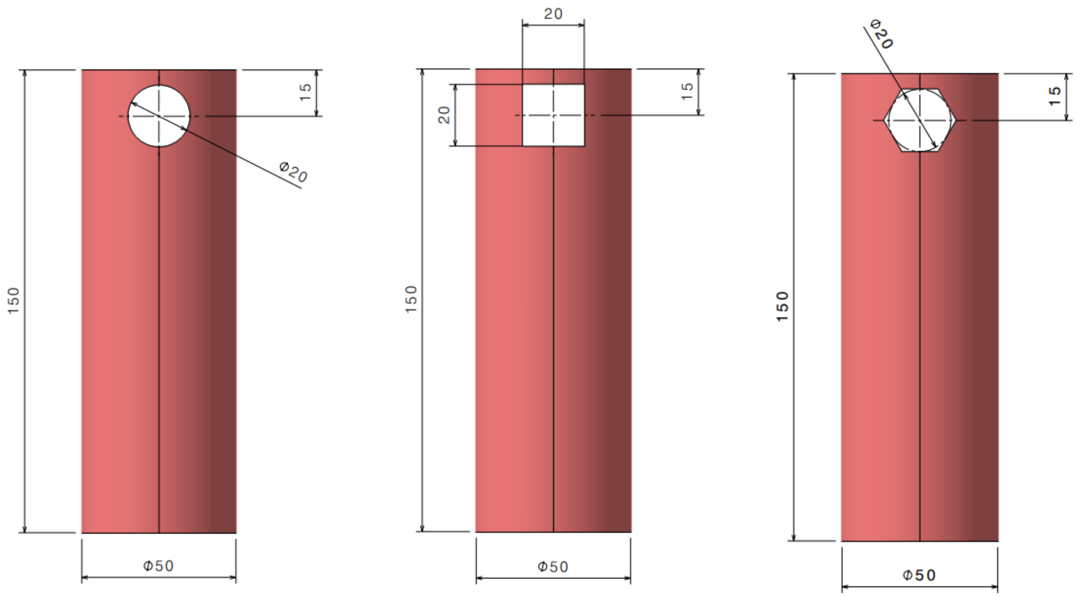

(a) (b) (c)

Figure 1: Thin-walled tubes with different shapes of cutout: (a) circular, (b) square, and (c) hexagon. Unit is in mm.

2.2 Numerical Modelling

The energy absorption characteristics of thin-walled tubes impacted under axial loading conditions were conducted using the finite element (FE) model, which is Ansys LS-PrePost version 4.7.7 software. In order to ensure the accuracy of the FE results, the development of the FE model in this study is imitated and compared with the previous study conducted by Ahmad et al. [13]. Figure 2 shows the FE model comprised of 3 main parts: thin-walled tube, moving mass, and stationary mass. The straight circular tube's length, radius, and thickness were 50.73 mm, 69.84 mm, and 0.58 mm, respectively. Besides that, for moving and stationary masses, the thickness was 2 mm while the length and width were set as 80 mm, respectively. For lateral motion, the moving mass was allowed to travel in the direction of the load axis only at an initial velocity, v_0 of 3.38 m/s, while the stationary mass was a constraint in all directions. In addition, all moving and stationary masses were also constrained in all rotational motions.

Eight node solid elements with a constant stress solid element formulation and a 10 mm mesh size are used to simulate the moving and stationary masses. The Belytschko-Tsay shell element formulation with five integration points across the thickness is used to create the tube. Four-node quadrilateral shell elements are appropriate for large strain analysis and are used to generate the tube mesh. Based on prior mesh convergence research done by Ahmad et al. [14], a shell element of 2.0 to 2.1 mm in size was used for the tube. The interface between the moving mass and the tube is created by utilizing "auto nodes to surface" contact. In order to prevent lateral motions, the moving mass is designated as the master part, while the tube is defined as the slave part, with static and dynamic friction coefficients of 0.2 and 0.1, respectively. The same contact type is used at the tube and stationary mass interface, with static and dynamic friction coefficients of 0.3 and 0.2, respectively.

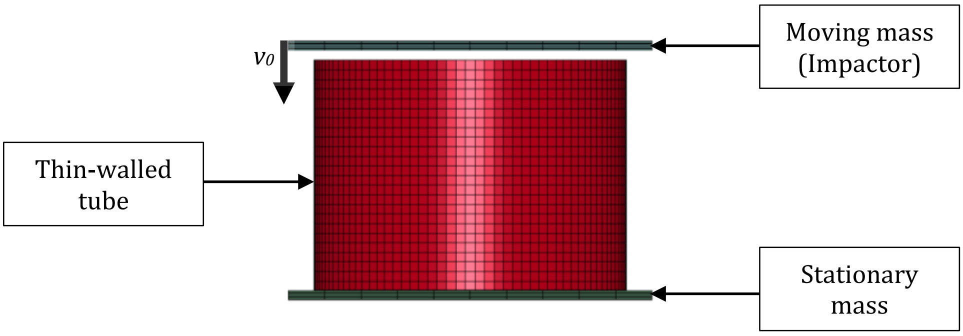

Figure 2: Configuration of moving mass, tube, and stationary mass in FE model.

A rigid material model (Material Model 020) has been assigned to both moving and stationary mass. This material model provides proper actions to turn the solid element parts into a rigid body [15]. Besides that, the aluminum alloy tube was modeled using material model 024 (piecewise linear plasticity) with the following mechanical properties: Young's modulus E = 68.9 GPa, initial yield stress σ_y = 276 MPa, Poisson's ratio v = 0.33, and mass density ρ = 2.7 g/cm^3 [14]. Piecewise linear plasticity model is based on the mathematical definitions of both work hardening and strain rate sensitivity. The Cowper-Symonds constitutive equation, which relates the dynamic and static yield stress as the strain rate effect is given by:

$$\sigma_y = \left[1 + \left(\frac{\dot{\varepsilon}}{C}\right)^{\frac{1}{p}}\right]\sigma_0 \quad (1)$$

where σ_y is the dynamic yield stress, $\dot{\varepsilon}$ is the strain rate, σ_0 is the static yield stress, and C and p are the strain rate parameters of the Cowper-Symonds material model. Based on prior work, aluminum alloy AA6061-T6 was discovered to be strain rate sensitive under dynamic loading [16]. Thus, the values of C and p for aluminum alloy AA6061-T6 are taken as 6400 and 4, respectively. The values of the effective plastic strain and the effective plastic stress for the quasi-static loading of the aluminum alloy AA6061-T6 employed in the material model are provided in Table 2.

Table 2: Effective plastic strain and effective plastic stress data for aluminum alloy AA6061-T6 [16].

Effective plastic strain (mm/mm)	0.000	0.010	0.015	0.020	0.030	0.040	0.060	0.080
Effective plastic stress (MPa)	276	280	286	292	304	317	335	350

The results obtained from the current FE model were compared with the experimental data to ensure that the current FE model developed in this study is trustworthy. To validate the FE model, the actual geometry, material, boundary, and initial condition for the specimens were taken from the actual experiment conducted by Ahmad et al. [13]. Figure 3 compares the deformed shape between the FE model and the previous experiment when impacted by a rigid body. The shape of the deformed tubes obtained from the FE model was almost similar to the experiment, although there is a different location on the tube's deformation. A single fold was obtained in both experiment and the FE model. In addition, the comparison between the experiment and FE also considers the results of maximum compression length, total energy absorption, and initial peak load, as listed in Table 3. There are a few differences between the FE model and the experimental result, with most of the results having recorded a very small percentage of errors between these methods. Although there is some disagreement between the FE model and the experimental result, these errors are still acceptable, considering this is a dynamic event. As the results showed an excellent correlation between the FE model and the experimental, thus the validated FE model is chosen to be applied in future studies.

(a) (b)

Figure 3: Comparison of shape deformation of a tube between (a) FE model and (b) previous experiment [13].

Table 3: Simulation and experiment result.

Factor	Experiment (Mat et al., 2019)	FE models	Percentages error
Max compression length (mm)	14.25	13.41	5.88
Total energy absorption (J)	106.93	114.29	6.44
Initial peak load (kN)	13.25	13.89	4.61

3. RESULTS AND DISCUSSION

The effect of size, shape, location and the number of cutouts on the square and circular thin-walled tubes will be discussed in this section. For comparison purposes, all specimens with similar thickness, diameter, and length are also impacted under a similar impact speed, as listed in Table 1. The results of energy absorption characteristics will be the outcome of the finding. It is desired to obtain a good energy absorption characteristic by achieving the highest value of energy absorption (EA) and specific energy absorption (SEA), the lowest value of initial peak load (IPL), and the unity value of crush force efficiency (CFE).

3.1 The effects of cutout size on energy absorption characteristics

The circular and square tubes with similar lengths, thicknesses, and diameters are used as the specimens in this section. A circular cutout has been created in the middle of the tube. In order to study the effect of the cutout size on the energy absorption characteristics, three different sizes of cutout diameter have been used, which are 14 mm, 20 mm, and 25 mm, respectively. Figure 4 shows the comparison of energy absorption characteristics for different shapes of tubes and different sizes of cutouts created in the middle of the tube. In terms of tube shape, circular tubes always provide superior energy absorption characteristics. It has been proved that the results of IPL, CFE, and SEA of the circular tube are always better than that of a square tube at any size of the cutout, except for the result of EA. By comparing to the square tube, the results of CFE and SEA can be increased up to 29% and 14%, respectively, when using the circular tube. Moreover, IPL also can be reduced by up to 68% when using the circular tube compared to the square tube. This finding is similar to the tubes without cutouts conducted in previous literature [4, 17]. This may be primarily caused by the fact that in square tubes, significant deformation is concentrated in areas close to the corners.

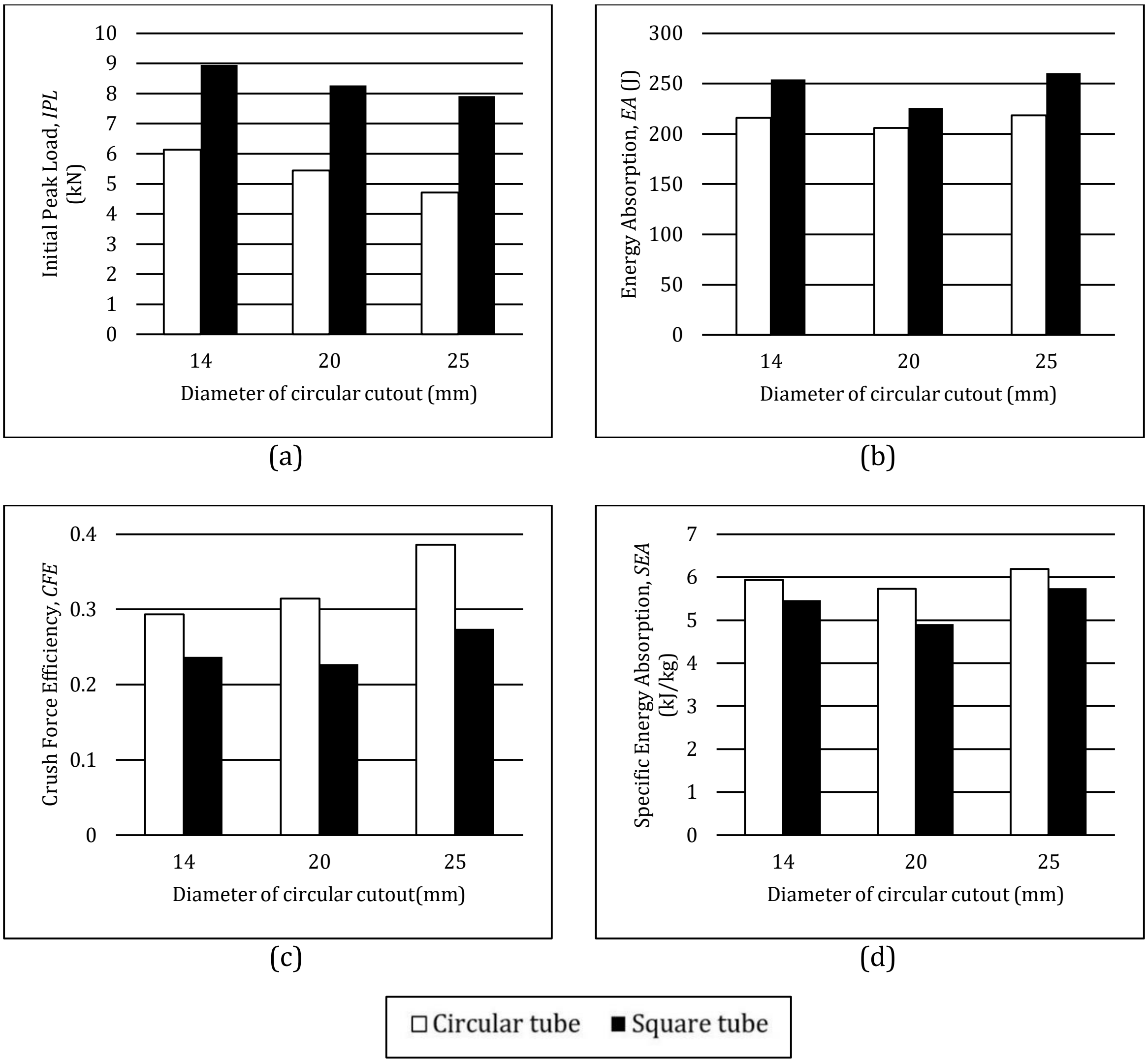

Figure 4: Effects of cutout size on (a) initial peak load, IPL, (b) energy absorption, EA, (c) Crush force efficiency, CFE, and (d) specific energy absorption, SEA of circular and square tubes. The cutout is circular and created in the middle of the tube.

Besides that, introducing a cutout to the tube has successfully improved the results of IPL and CFE. The value of IPL can be decreased by 23% when increasing the cutout size from 14 to 25 mm on a circular tube. In addition, CFE also can be improved by 32% when increasing the size of the cutout from 14 mm to 25 mm on a circular tube. However, increasing the cutout size gives insignificant results on the EA and SEA. Thus, a bigger cutout size is preferred as it can improve the value of IPL and CFE without reducing the value of EA and SEA. However, it is suggested that a wider range of sizes can be explored in future studies.

3.2 The effects of cutout shape and cutout location on energy absorption characteristics

In this section, the effect of the cutout shape and location on the thin-walled tube towards the energy absorption characteristics will be discussed. As the circular tube performed better than the square tube discussed in Section 3.2, thus, this tube will be selected. In addition, from the finding in Section 3.2, the largest cutout diameter (25 mm) is applied to the whole tube, as shown in Figure 5. Three different locations of the cutout have been selected, which are at the top, middle and bottom, as shown in Figure 5. For the cutout at the top location, the distance from the center of the cutout to the top of the tube is 15 mm. For the cutout at the bottom location, the distance from the bottom of the tube to the center of the cutout is also 15 mm. For the cutout in the middle, the distance from the center of the cutout is 75 mm from both the top and bottom of the tube, respectively. Moreover, three different shapes of the cutout, which are circular, square, and hexagon, are applied to analyze the effect of cutout shape on crashworthiness.

Figure 6 shows the results of energy absorption characteristics when varying the cutout location and shapes. From the result, applying the cutout at the top or bottom of the tube gives more advantages than applying the cutout at the middle of the tube. The high value of EA can observe in its CFE and SEA in Figure 3(b)-(d), respectively. In addition, the cutout location does not give significant results on the value of IPL, where the values are almost similar at any cutout location except for the circular cutout. Particularly, the cutout at the top of the tube provides the most excellent results compared to the bottom tube. Moving the cutout closer to the impact end could reduce the buckling strength of the tube at the impact end, making it easy to initiate local buckling and hence the folding.

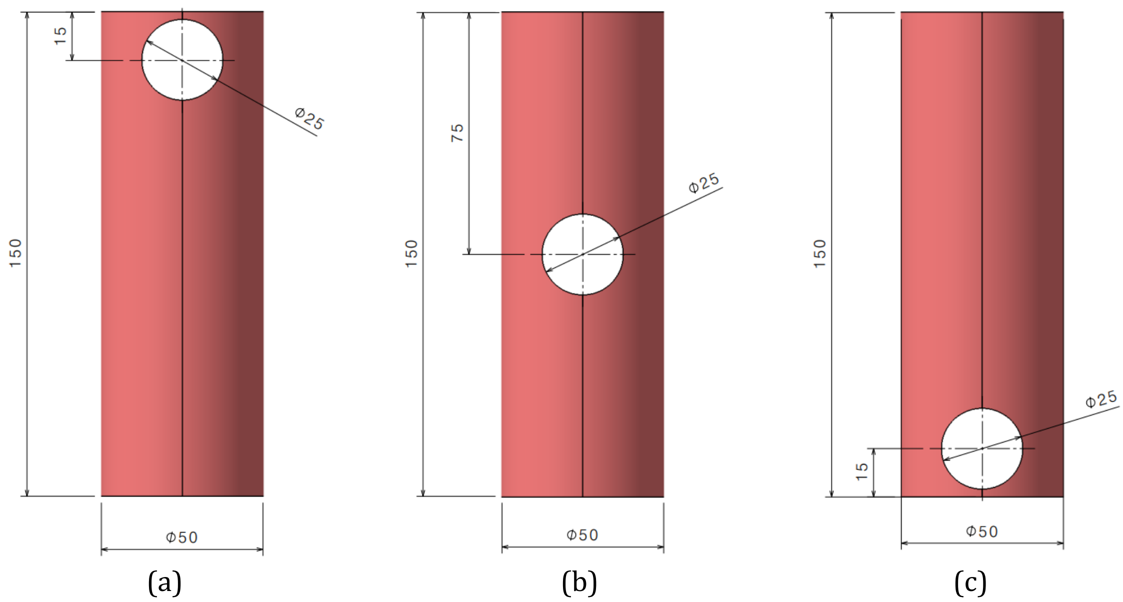

Figure 5: Thin-walled tubes with different locations of cutout: (a) Top, (b) Middle, and (c) Bottom. Unit is in mm.

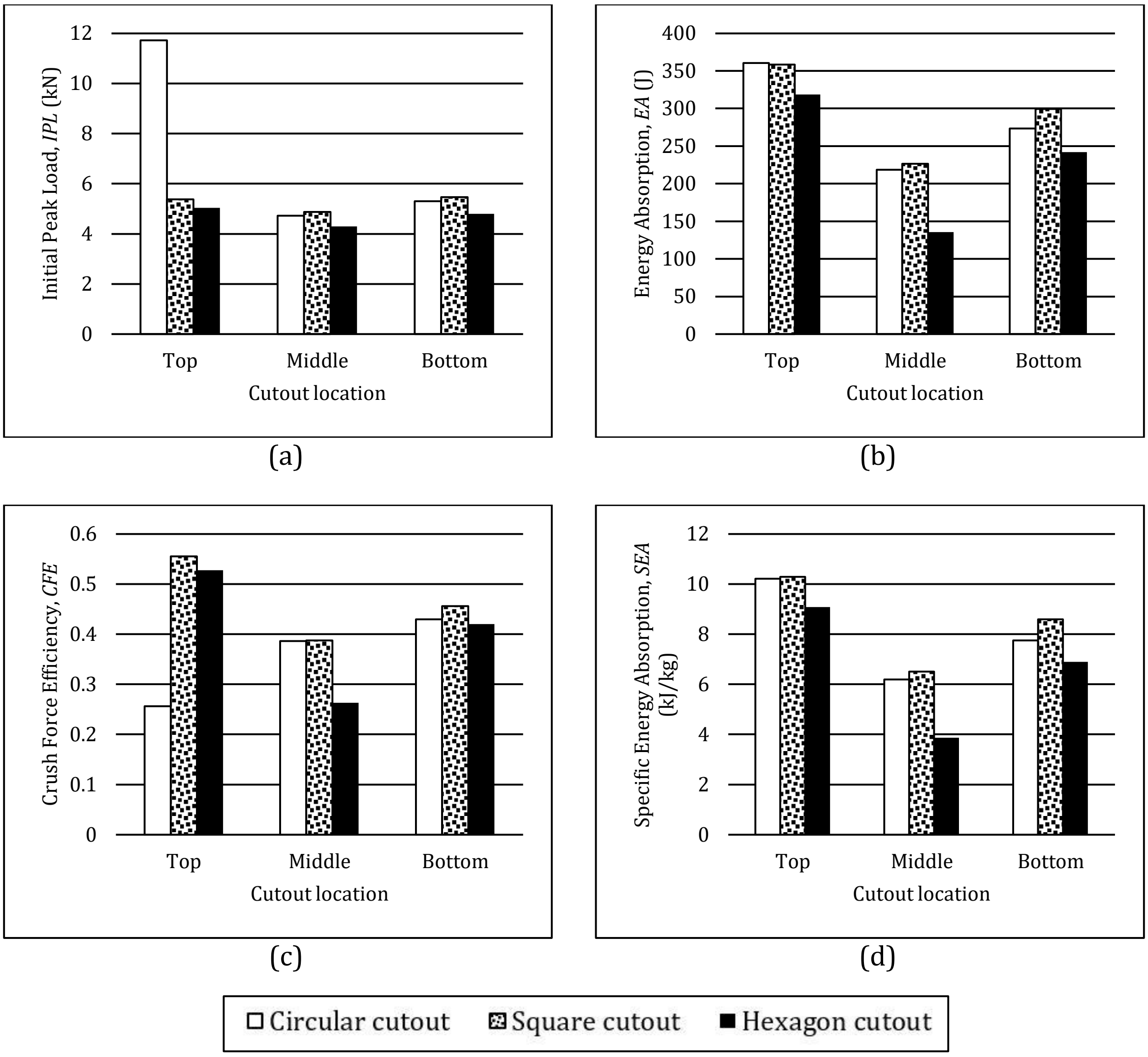

Figure 6: Effects of cutout shape and cutout location on (a) initial peak load, IPL, (b) energy absorption, EA, (c) Crush force efficiency, CFE, and (d) specific energy absorption, SEA of the circular tube with 25 mm of cutout diameter.

On the other hand, in terms of cutout shape, most square cutout shapes provide the best results of EA, CFE, and SEA, followed by circular and hexagon tubes. However, opposite findings were obtained for the IPL. It should be noted that this finding is obtained due to IPL being related to CFE without considering the parameters of the mean crushing force. Moreover, the number and corners of the hexagon shape may affect these results. In addition, the orientation of the square shape of the cutout could be investigated in future studies.

3.3 The effects of the number of cutouts on energy absorption characteristics

In this section, the number of cutouts on a thin-walled tube has varied from a single cutout to five, as shown in Figure 7. The cutouts having a diameter of 20 mm, are positioned on the wall at an equal distance from the bottom. The distance between the top end of the tube is 15 mm, and the center of the top end hole is 75 mm. Most of the tubes deformed with a mixed mode pattern except for the cutouts with four holes, which resulted in a progressive diamond mode.

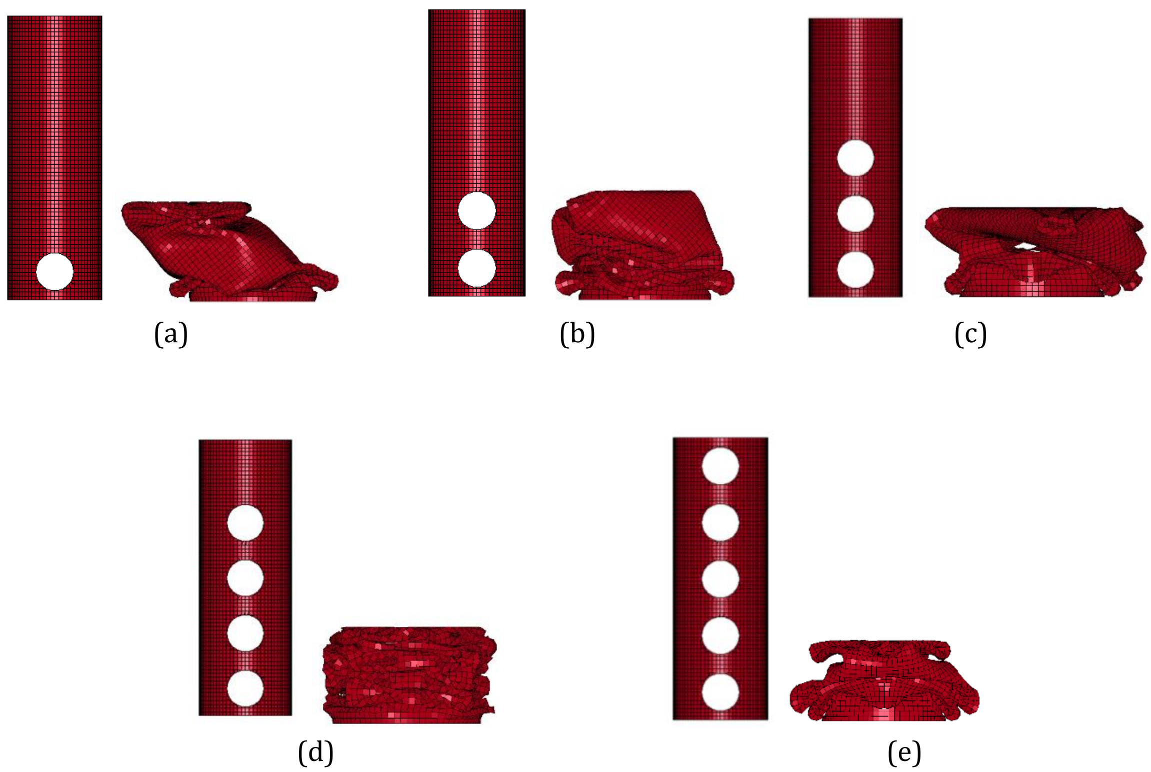

Figure 7: Deformed shapes of tubes with different numbers of cutouts: (a) One circular cutout on a circular tube (b) Two circular cutouts (c) Three circular cutouts (d) Four circular cutouts (e) Five circular cutouts.

The results of energy absorption characteristics for the tube with different numbers of cutouts are shown in Figure 8. For the IPL result, the value of IPL could be reduced to 8.9 % when increasing from 1 to 3 holes of cutouts. However, IPL increased when using four cutouts but resulted in an optimum IPL when applying five cutouts. Besides, increasing the number of cutouts to four holes. Besides that, the results of EA, CFE, and SEA are highest when using four cutouts. This result was obtained due to the tube being deformed in progressive buckling mode, as shown in Figure 7(d).

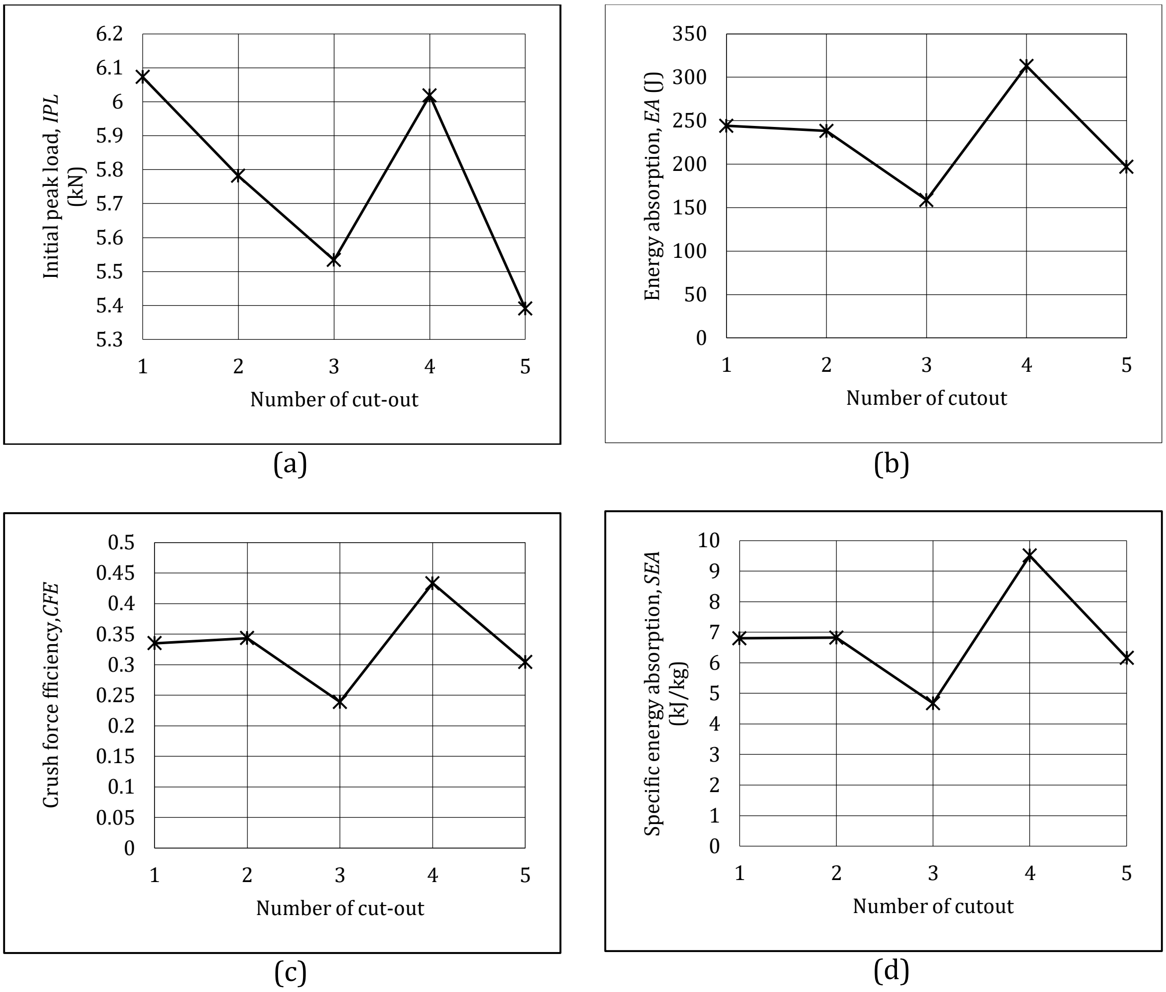

Figure 8: Effects of the number of the cutout on the thin-walled tubes to (a) initial peak load, IPL, (b) energy absorption, EA, (c) crush force efficiency, CFE, and (d) specific energy absorption.

4. CONCLUSION

Overall, the effects of the cutout on the surface of thin-walled structures have been discussed in this study. The validated FE model has been used to simulate the impact of tubes under axial loading. A comparison has been made between crushing between circular and square tubes, and it has been found that a circular tube provides better energy absorption characteristics compared to a square tube. It has been proved that the results of the IPL, CFE, and SEA of the circular tube are always better than the square tube at any size of the cutout, except for the result of EA. In terms of cutout size, a bigger cutout size is preferred as it can improve the value of IPL and CFE without reducing the value of EA and SEA. Besides that, applying the cutout at the top or bottom of the tube can improve better results of EA, CFE, and SEA than applying the cutout at the middle of the tube. Particularly, the cutout at the top of the tube provides the most excellent results compared to the bottom tube. On the other hand, in terms of cutout shape, most of the square cutout shape provides the best results of EA, CFE, and SEA, followed by circular and hexagon tubes. Besides that, the results of EA, CFE, and SEA are highest when applying four cutouts. It is suggested that a wider range of sizes and orientations can be explored in future studies.

ACKNOWLEDGEMENTS

We acknowledged the financial support was from the Malaysian Ministry of Education through Fundamental Research Grant Scheme (FRGS) no: FRGS/1/2020/TK0/UNIMAP/02/9 (UniMAP Project Code: 9003-00806).

REFERENCES

[1] World Health Organization, & United Nations Regional Commissions. Global Plan Decade of Action for Road Safety 2021–2030, (2021).

[2] Magliaro, J., Altenhof, W., & Alpas, A. T. A review of advanced materials, structures and deformation modes for adaptive energy dissipation and structural crashworthiness. Thin-Walled Structures, vol 180, (2022) p. 109808.

[3] San Ha, N., & Lu, G. A review of recent research on bio-inspired structures and materials for energy absorption applications. Composites Part B: Engineering, vol 181, (2020) p. 107496.

[4] Baroutaji, A., Sajjia, M., & Olabi, A. G. On the crashworthiness performance of thin-walled energy absorbers: recent advances and future developments. Thin-Walled Structures, vol 118, (2017) p. 137-163.

[5] Luo, X., Xu, J., Zhu, J., Gao, Y., Nie, L., & Li, W. A new method to investigate the energy absorption characteristics of thin-walled metal circular tube using finite element analysis. Thin-Walled Structures, vol 95, (2015) p. 24-30.

[6] Fang, J., Gao, Y., Sun, G., Zheng, G., & Li, Q. Dynamic crashing behavior of new extrudable multi-cell tubes with a functionally graded thickness. International Journal of Mechanical Sciences, vol 103, (2015) p. 63-73.

[7] Nia, A. A., & Parsapour, M. Comparative analysis of energy absorption capacity of simple and multi-cell thin-walled tubes with triangular, square, hexagonal and octagonal sections. Thin-Walled Structures, vol 74, (2014) p.155-165.

[8] San Ha, N., & Lu, G. Thin-walled corrugated structures: A review of crashworthiness designs and energy absorption characteristics. Thin-Walled Structures, vol 157, (2020) p. 106995.

[9] Barzigar, S. S., Ahmadi, H., & Liaghat, G. An analytical investigation on the crushing behavior of thin-walled tubes filled with a foam with strain hardening region. Thin-Walled Structures, vol 182, (2023) p. 110169.

[10] Taştan, A., Acar, E., Güler, M. A., & Kılınçkaya, Ü. Optimum crashworthiness design of tapered thin-walled tubes with lateral circular cutouts. Thin-Walled Structures, vol 107, (2016) p. 543-553.

[11] Kathiresan, M. Influence of shape, size and location of cutouts on crashworthiness performance of aluminium conical frusta under quasi-static axial compression. Thin-Walled Structures, vol 154, (2020) p. 106793.

[12] Song, J., Chen, Y., & Lu, G. Light-weight thin-walled structures with patterned windows under axial crushing. International Journal of Mechanical Sciences, vol 66, (2013) pp. 239-248.

[13] Ahmad, M., Ismail, K. A., Hanid, M. H. M., Mat, F., & Roslan, A. M. Modification of the design of circular thin-walled tubes to enhance dynamic energy absorption characteristics: Experimental and finite element analysis. In IOP Conference Series: Materials Science and Engineering, vol 917, issue 1 (2020) p. 012027.

[14] Ahmad, M., Ismail, K. A., & Mat, F. Convergence of finite element model for crushing of a conical thin-walled tube. Procedia Engineering, vol 53, (2013) pp. 586-593.

[15] Hallquist, J., LS-DYNA® theory manual, no. March (2006).

[16] Norman Jones, Structural Impact. Australia: Cambridge University Press, (1989).

[17] Tang, Z., Liu, S., & Zhang, Z. Analysis of energy absorption characteristics of cylindrical multi-cell columns. Thin-Walled Structures, vol 62, (2013) pp. 75-84.